Revista Mexicana de Ciencias Forestales Vol. 16 (92)
Noviembre - Diciembre (2025)

DOI: 10.29298/rmcf.v16i92.1579

Research article

Comparison of models to estimate *DBH* of *Pinus hartwegii* Lindl. with LiDAR data

Comparación de modelos para estimar el diámetro normal de *Pinus hartwegii* Lindl. con datos *LiDAR*

Fabián Islas-Gutiérrez[1*], Vidal Guerra-De la Cruz[2], Hugo Ramírez-Maldonado[3], Enrique Buendía-Rodríguez[1], Tomás Pineda-Ojeda[1], Eulogio Flores-Ayala[1]

Fecha de recepción/Reception date: 4 de junio de 2025
Fecha de aceptación/Acceptance date: 13 de agosto de 2025

[1]Instituto Nacional de Investigaciones Forestales, Agrícolas y Pecuarias (INIFAP), Campo Experimental Valle de México. México
[2]Instituto Nacional de Investigaciones Forestales, Agrícolas y Pecuarias (INIFAP), Sitio Experimental Tlaxcala, México
[3]Universidad Autónoma Chapingo, División de Ciencias Forestales, México.

*Autor para correspondencia; correo-e: islas.fabian@inifap.gob.mx
*Corresponding author; e-mail: islas.fabian@inifap.gob.mx

Abstract

DBH is a fundamental variable in forest management. Airborne LiDAR sensors have demonstrated their usefulness in supporting forest inventories; however, it is not possible to directly measure *DBH* with them. *Pinus hartwegii* is the main tree species in the highlands of Mexico, providing important ecosystem services such as carbon sequestration and rainwater infiltration. The objective of this study was to design an equation to estimate the *DBH* of individual *P. hartwegii* trees, based on tree measurements obtained from airborne LiDAR data. 85 identifiable *P. hartwegii* trees were selected on a digital orthomosaic and their UTM coordinates were recorded. With these coordinates they were located in the field and their *DBH*, total height, height to crown base and crown diameter were measured. They were located in a LiDAR point cloud and the same variables were measured as in the field, except for the *DBH*. 29 models reported in the literature were evaluated to estimate normal diameter, using 7 independent variables obtained from the LiDAR data. The best model (M27) is an adaptation of the one known in the literature as Gompertz. It obtained an R^2adj=0.884, *RMSE*=6.5 cm. The validation results indicate that its estimates are adequate for calculating the *DBH* from the total height and crown diameter obtained from LiDAR data.

Key words: Airborne, individual trees, LiDAR, *Pinus hartwegii* Lindl., regression, remote sensing.

Resumen

El diámetro de los árboles es una variable fundamental en el manejo forestal. Los sensores *LiDAR* aerotransportados han demostrado su utilidad en el apoyo de inventarios forestales; sin embargo, con ellos no es posible medir directamente el diámetro de los árboles. *Pinus hartwegii* es la principal especie arbórea de las partes altas de México, aporta importantes servicios ecosistémicos como la captura de carbono e infiltración del agua de lluvia. El objetivo del presente estudio fue diseñar una ecuación que permita estimar el diámetro normal de árboles individuales de *P. hartwegii*, a partir de medidas del arbolado obtenidas de datos *LiDAR* aerotransportados. Sobre un ortomosaico digital se seleccionaron 85 árboles de *P. hartwegii* que fueran identificables y se registraron sus coordenadas UTM; con estas se localizaron en campo y se les midió el diámetro normal, la altura total, la altura de fuste limpio y el diámetro de copa. Se ubicaron en una nube de puntos *LiDAR* en la que se midieron las mismas variables que en campo, excepto el diámetro normal. Se evaluaron 29 modelos consignados en la literatura para estimar el diámetro normal y se utilizaron siete variables independientes de los datos *LiDAR*. El mejor modelo (M27) es una adecuación conocida como *Gompertz*. Se obtuvo un R^2ajd = 0.884, *RECM* = 6.5 cm. Los resultados de la validación indican que sus estimaciones son acertadas para calcular el diámetro normal en función de la altura total y el diámetro de copa a partir de datos *LiDAR*.

Palabras clave: Aerotransportado, árboles individuales, *LiDAR*, *Pinus hartwegii* Lindl., regresión, sensores remotos.

Introduction

T Normal diameter is one of the most widely used dasometric variables in forest inventories (Fu et al., 2018), not only for the study of individual trees but also for the study of forest structure (Hulshof et al., 2015). Among other applications, it allows for the estimation of other variables such as total height (Ng'andwe et al., 2019), crown diameter (Ogana, 2019), volume (Valverde et al., 2022), as well as biomass and carbon in the aboveground part of the tree (Montes de Oca-Cano et al., 2020).

Remote sensing has demonstrated its benefits in different areas of knowledge, both for classification and change detection (Ma et al., 2019). In the forestry sector, it has been used for biodiversity detection (Wang & Gamon, 2019), as a support for forest inventories (Lara-Vásconez & Chamorro-Sevilla, 2018), and, more generally, in forest management (Ancira-Sánchez & Treviño-Garza, 2015). Passive sensors that record data in multispectral images have been widely used. However, in recent years, active sensors such as airborne LiDAR (Light Detection and Ranging) have

gained relevance because they allow the heights of objects to be determined and, therefore, allow 3D data analysis (Guo et al., 2021; Reutebuch et al., 2005).

Measuring crown diameter and the height of individual trees is feasible with LiDAR data obtained from airborne devices (Galvincio & Popescu, 2016; Shiota et al., 2017). In the case of normal diameter, direct measurement is not possible (Allouis et al., 2013) because the tree canopy obstructs the passage of most laser pulses. However, some authors such as Bi et al. (2012) and Hall et al. (1989) have suggested that, if the normal diameter can be used to estimate other tree characteristics, then it is also possible to obtain an inverse function that uses some tree characteristics measured with remote sensors to estimate the normal diameter. Thus, Hall et al. (1989) worked with total height and crown area derived from aerial photographs as explanatory variables for normal diameter. Liu et al. (2017) used crown area extracted from images from unmanned aerial vehicles.

LiDAR data have also been incorporated into this type of research; Fu et al. (2018) used height and projection of the crown area, while Yang et al. (2020) were based on height, crown width and crown area. With this premise, Islas-Gutiérrez et al. (2023), in an exploratory study, evaluated two linear and two power models to estimate the normal diameter of *Pinus hartwegii* Lindl. using LiDAR data; their results suggest further searching, based on the biometric models reported in literature, for a model with better statistical fits.

Pinus hartwegii is the tree species that inhabits the highest areas of the Valley of Mexico, growing between 3 000 and 4 200 masl. It plays a relevant role in the provision of ecosystem services (Pérez-Suárez et al., 2022), and therefore must be protected with forest management that ensures its continued existence in the future. As a contribution to this goal, the objective of this study was to identify an equation that allows estimating the normal diameter of individual *Pinus hartwegii* trees, based on tree measurements obtained from airborne LiDAR data.

Materials and Methods

Study Area

The research was conducted in the forest areas of the *Tequexquináhuac*, *San Dieguito Xochimanca*, *Santa María Nativitas*, *San Pablo Ixayoc*, *and San Miguel Tlaixpan ejidos*, *Texcoco* municipality, State of Mexico, Mexico, located between the coordinates 19°24’33.24” and 19°26’18.53” N and 98°43’47.43” and 98°45’24.22” W (Figure 1), on a 500 ha area, with an average altitude of 3 570 m. The predominant climate is temperate-humid with summer rainfall, average temperatures between 10 and 14 °C, and average annual precipitation between 900 and 1 200 mm (Hernández-Ramírez et al., 2022).

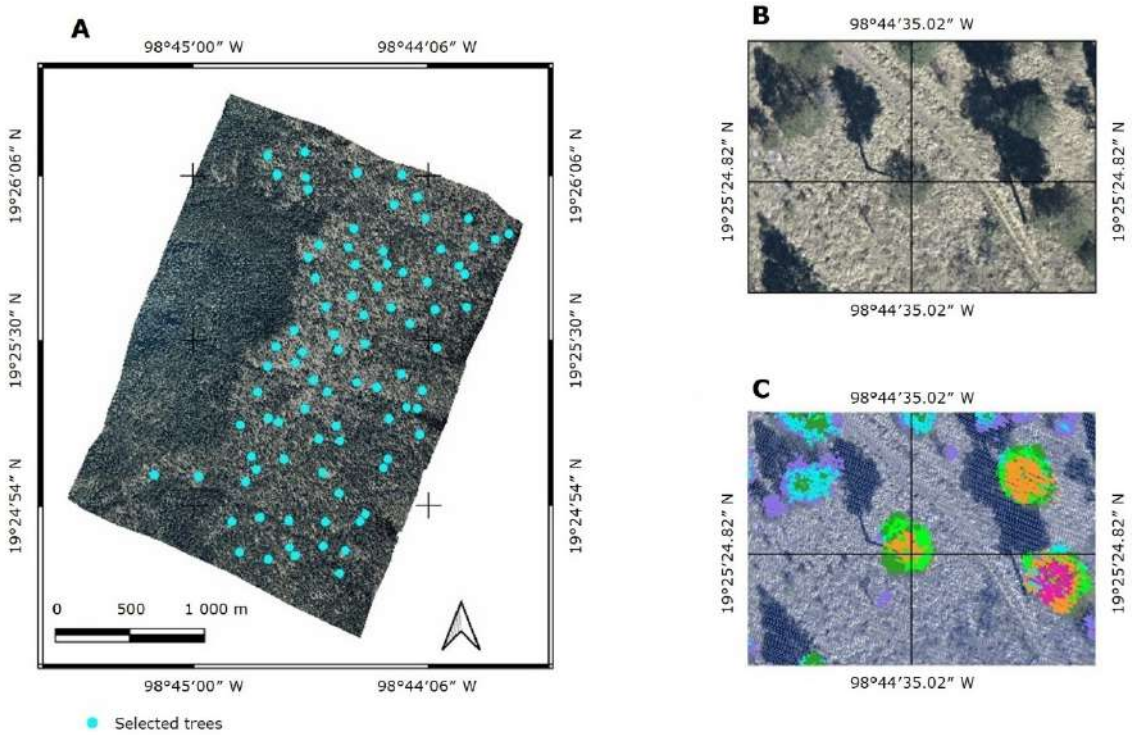

A = Tree location in the study area; B = Tree identified in the digital orthophoto; C = Tree identified in the LiDAR data.

Figure 1. Study area and tree location.

The tree vegetation is characterized by mature stands of the *Pinus* L., *Abies* Mill., and *Quercus* L. genera, of which *Pinus hartwegii* is the predominant species above 3 500 masl. Part of the study area is located within the *Iztaccíhuatl-Popocatépetl* National Park polygon, where timber harvesting is not allowed except for scientific collection, sanitation and domestic use (Comisión Nacional de Áreas Naturales Protegidas [Conanp], 2013).

Data collection

The LiDAR point cloud was obtained with a model ALS60 *Leica*® sensor mounted on a small aircraft. The flight was conducted at a speed of 167 km h^{-1} and an average altitude of 808 m, which allowed for a density of 8 points per m^2. During the same flight, aerial photographs were taken with a model RC30 *Leica*® camera. These photographs were used to create a digital orthomosaic with a spatial resolution of 10×10 cm.

From the orthomosaic, deployed in QGIS version 3.42 software (QGIS Development Team, 2024), 85 *Pinus hartwegii* trees distributed throughout the study area (Figure 1A) were selected that could be recognized in the field (Figure 1B), and their UTM coordinates were recorded.

Between January and March 2019, with the support of GNSS receivers (model eTrex 10 Garmin® and GPSMAP 78s Garmin®, both with a location error of ±3.65 m), the 85 trees were located in the field. The normal diameter (*ND*; cm) of each tree was measured using a model 349D Forestry Suppliers® diameter measure tape, the total height (*TH*; m) and bare stem height (*BSH*; m) were measured by using a model CI Gen 2 Haglöf® electronic clinometer, and the largest and smallest crown diameters were measured with a model HLF030 30-m Lufkin® fiberglass tape measure. The average crown diameter (*CD*; m) was calculated from these field-measured crown diameters.

Tree attributes derived from LiDAR

Using FUSION/LDV version 4.61 software (McGaughey, 2024), the digital terrain model was generated and used to normalize the LiDAR point cloud. Tree coordinates were used to locate them in the point cloud (Figure 1C). Each tree was measured for total height (*THL*; m), bare stem height (*BSHL*; m) and the largest and smallest crown diameters. The average crown diameter (*CDL*; m) was calculated from these two measurements. In addition, the variables suggested by Oono and Tsuyuki (2018) were generated: crown length (*LCL*) with Equation 1, crown ratio (*RCL*) with Equation 2, lateral crown surface area (*SCL*) with Equation 3 and LiDAR crown volume (*VCL*) with Equation 4. For the calculation of *SCL* and *VCL*, it was assumed that the crown of the trees is conical.

$$LCL = THL - BSHL \quad (1)$$

$$RCL = \frac{LCL}{THL} \quad (2)$$

$$SCL = n\frac{CDL}{2}\sqrt{\left(\frac{CDL}{2}\right)^2 + LCL^2} \quad (3)$$

$$VCL = \frac{n\left(\frac{CDL}{2}\right)^2 LCL}{3} \quad (4)$$

Where:

n = Number of observations

Statistical analysis

To verify the agreement between field measurements and LiDAR data, the Pearson correlation coefficient was calculated, and a difference-of-means test was performed between them (Ott & Longnecker, 2010).

From the set of trees, an 80 % sample was randomly selected and used to fit the models. The remaining percentage (20 %) was used to validate the model with the best fit statistics. At the beginning of the statistical analysis, Pearson correlation coefficients were calculated among the seven LiDAR variables and *ND*. Based on this analysis, the three LiDAR variables with the highest correlation with *ND* and the lowest correlation between them were selected as independent variables for the regression models. From the literature, power models and modifications of the well-known models such as Richards, Hossfeld I, Schumacher and Gompertz were selected. Thus, thirteen types of models were evaluated (Table 1). In the case of the model proposed by Islas-Gutiérrez et al. (2023), only the version with two explanatory variables was considered, as it obtained the best fit statistics.

Table 1. Structure of models used to estimate the normal diameter.

Model	Source
$ND = \beta_0\, x_1^{\beta_1}\, x_2^{\beta_2} + \varepsilon$	Islas-Gutiérrez et al. (2023)
$ND = \beta_0\, e^{-(\beta_1 x_1)} + \varepsilon$	Yang et al. (2020)
$ND = \beta_0\, e^{-(\beta_1 x_1 + \beta_2 x_2)} + \varepsilon$	Yang et al. (2020)
$ND = \beta_0\, e^{-(\beta_1 x_1 + \beta_2 x_2 + \beta_3 x_3)} + \varepsilon$	Yang et al. (2020)
$ND = \frac{x_1^2}{(\beta_0 + \beta_1\, x_1)^2} + \varepsilon$	Hernández et al. (2020)
$ND = \frac{x_1^2}{(\beta_0 + \beta_1\, x_1 + \beta_2\, x_2)^2} + \varepsilon$	Hernández et al. (2020)
$ND = \frac{x_1^2}{(\beta_0 + \beta_1\, x_1 + \beta_2\, x_2 + \beta_3\, x_3)^2} + \varepsilon$	Hernández et al. (2020)
$ND = \beta_0 e^{\left[-\left(\beta_1 \frac{1}{x_1}\right)\right]} + \varepsilon$	Hernández et al. (2020)
$ND = \beta_0 e^{\left[-\left(\beta_1 \frac{1}{x_1} + \beta_2 \frac{1}{x_2}\right)\right]} + \varepsilon$	Hernández et al. (2020)
$ND = \beta_0 e^{\left[-\left(\beta_1 \frac{1}{x_1} + \beta_2 \frac{1}{x_2} + \beta_3 \frac{1}{x_3}\right)\right]} + \varepsilon$	Hernández et al. (2020)
$ND = \beta_0\, e^{[\beta_1 e^{(\beta_2 x_1)}]} + \varepsilon$	Hernández-Cuevas et al. (2018)
$ND = \beta_0\, e^{[\beta_1 e^{(\beta_2 x_1 + \beta_3 x_2)}]} + \varepsilon$	Hernández-Cuevas et al. (2018)
$ND = \beta_0\, e^{[\beta_1 e^{(\beta_2 x_1 + \beta_3 x_2 + \beta_4 x_3)}]} + \varepsilon$	Hernández-Cuevas et al. (2018)

ND = Normal diameter; β_0, β_1, β_2, β_3 and β_4 = Parameters of the model; x_1, x_2 and x_3 = Predictor variables; ε = Random error.

In order to establish the best model, the Coefficient of determination adjusted by the number of parameters (R^2ajd), the Root Mean Square Error (*RMSE*), the value of the *Akaike* information criterion (*AIC*) were considered, in addition to meeting the assumptions of normality in the distribution of the residuals and homogeneity of variance. In order to facilitate the selection process of the adjusted models based on the first three statistics, the scoring procedure proposed by Tamarit-Urías et al. (2014) was followed. Likewise, the significance ($p<0.05$) of the regression parameters in each model was determined as another important criterion. The model adjustment was performed in SAS® version 9.3 (SAS Institute Inc., 2011).

The Intraclass correlation coefficient (*ICC*) (Martínez-Pérez & Pérez-Martín, 2023) and a paired-samples *t*-test were used to validate the model. Unlike Pearson's correlation coefficient, which assesses the strength of the linear association between two variables, the *ICC* evaluates the agreement of measurements (Fau et al., 2020). In line with Koo and Li (2016), a two-factor mixed-effects model with a single measure and absolute agreement was used. Calculations were performed using the *icc* command from the irr package and the *t.test* command, both from R software version 4.4.3 (R Core Team, 2025).

Results and Discussion

The tree sample used in this study was distributed within a range of normal diameters between 9 and 90 cm, total heights between 5 and 33 m, stem heights between 1.5 and 20 m, and crown diameters between 1.9 and 15.5 m. The LiDAR variable values established correlations greater than 0.95 with field values (Figure 2). Regarding the means tests, the null hypothesis was not rejected for the

variables total height (p=0.558) and crown diameter (p=0.031), but this was not the case for the variable bare stem height, which was highly significant, thus rejecting the hypothesis of equality (p<0.001).

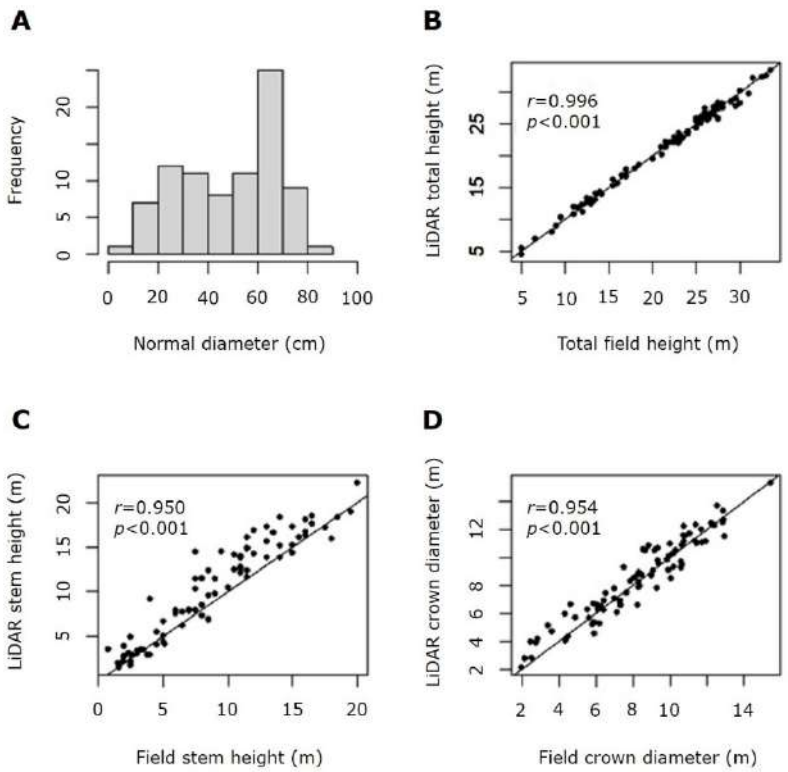

A = Frequency histogram of normal diameter; B = Total height correlation; C = Stem height correlation; D = Crown diameter correlation.

Figure 2. Dispersion and correlations between field and LiDAR data.

Based on the correlation analysis between the LiDAR predictor variables and the response variable, *THL*, *CDL* and *SCL* showed the highest correlations (r≥0.8; p<0.01) with *ND* (Figure 3). However, *SCL* showed a high correlation with *CDL* (r=0.911; p<0.001) and *VCL* (r=0.982; p<0.001), which suggests a potential

autocorrelation problem with these variables. Therefore, *SCL* was ruled out as a possible predictor of *ND*. *VCL* was the next most highly correlated variable with *ND* (r=0.764; p<0.001); however, it has a high correlation with *CDL* (r=0.908; p<0.001), so it was also discarded. The variable *BSHL* has a Correlation coefficient with *ND* of 0.713 (p<0.001), and the correlation with the other possible predictor variables is less than 0.9. Therefore, *BSHL* was considered the third independent variable to include in the models that estimate *ND*.

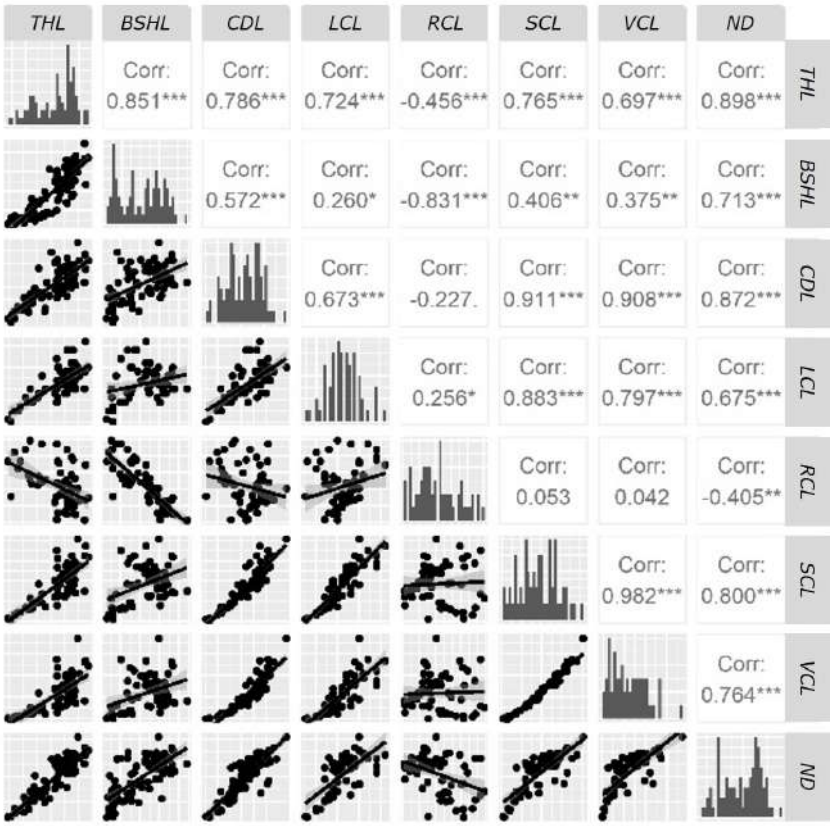

THL = LiDAR total height; *BSHL* = LiDAR stem height; *CDL* = LiDAR crown diameter; *LCL* = LiDAR crown length; *RCL* = LiDAR crown ratio; *SCL* = LiDAR crown area; *VCL* = LiDAR crown volume; *ND* = Normal diameter; Corr. = Correlation; *p<0.05, **p<0.01, ***p<0.001.

Figure 3. Dispersion and Pearson correlation coefficients of the normal diameter with each of the variables measured in the LiDAR data.

It should be noted that the Pearson correlation coefficient estimates linear correlations, which are not necessarily those that occur between the predictor variables and the normal diameter. However, in the pre-adjustment phase, it constitutes an important approximation for identifying variables with potentially significant relationships in the modeling of normal diameter, which is why it has also been used for this purpose in other studies (Zhang et al., 2023).

Once the variables to be incorporated into the proposed models were selected (Table 1), a total of 29 equations were evaluated with the combinations of the defined predictor variables (Table 2).

Table 2. Assessed models to estimate the normal diameter of *Pinus hartwegii* Lindl.

ID	Model	ID	Model
M1	$ND = b_0\ THL^{b_1}\ CDL^{b_2}$	M16	$ND = b_0 e^{[-(b_1 \frac{1}{THL})]}$
M2	$ND = b_0\ e^{-(b_1 THL)}$	M17	$ND = b_0 e^{[-(b_1 \frac{1}{BSHL})]}$
M3	$ND = b_0\ e^{-(b_1 BSHL)}$	M18	$ND = b_0 e^{[-(b_1 \frac{1}{CDL})]}$
M4	$ND = b_0\ e^{-(b_1 CDL)}$	M19	$ND = b_0 e^{[-(b_1 \frac{1}{THL} + b_2 \frac{1}{BSHL})]}$
M5	$ND = b_0\ e^{-(b_1 THL + b_2 BSHL)}$	M20	$ND = b_0 e^{[-(b_1 \frac{1}{THL} + b_2 \frac{1}{CDL})]}$
M6	$ND = b_0\ e^{-(b_1 THL + CDL)}$	M21	$ND = b_0 e^{[-(b_1 \frac{1}{BSHL} + b_2 \frac{1}{CDL})]}$
M7	$ND = b_0\ e^{-(b_1 BSHL + CDL)}$	M22	$ND = b_0 e^{[-(b_1 \frac{1}{THL} + b_2 \frac{1}{BSHL} + b_3 \frac{1}{CDL})]}$
M8	$ND = b_0\ e^{-(b_1 THL + b_2 BSHL + b_3 CDL)}$	M23	$ND = b_0\ e^{[b_1 e^{(b_2\ THL)}]}$
M9	$ND = \frac{THL}{(b_0 + b_1 THL)^2}$	M24	$ND = b_0\ e^{[b_1 e^{(b_2\ BSHL)}]}$
M10	$ND = \frac{BSHL}{(b_0 + b_1 BSHL)^2}$	M25	$ND = b_0\ e^{[b_1 e^{(b_2\ CDL)}]}$

M11 $ND = \frac{CDL}{(b_0 + b_1 CDL)^2}$

M12 $ND = \frac{THL}{(b_0 + b_1 THL + b_2 CDL)^2}$

M13 $ND = \frac{THL}{(b_0 + b_1 THL + b_2 BSHL)^2}$

M14 $ND = \frac{THL}{(b_0 + b_1 BSHL + b_2 CDL)^2}$

M15 $ND = \frac{THL}{(b_0 + b_1 THL + b_2 BSHL + b_3 CDL)^2}$

M26 $ND = b_0\, e^{[b_1\, e^{(b_2\, THL + b_3\, BSHL)}]}$

M27 $ND = b_0\, e^{[b_1\, e^{(b_2\, THL + b_3\, CDL)}]}$

M28 $ND = b_0\, e^{[b_1\, e^{(b_2\, BSHL + b_3\, CDL)}]}$

M29 $ND = b_0\, e^{[b_1\, e^{(b_2\, THL + b_3\, BSHL + b_4 CDL)}]}$

ND = Normal diameter; *THL* = LiDAR total height; *BSHL* = LiDAR stem height; *CDL* = LiDAR crown diameter; b_0, b_1, b_2, b_3 and b_4 = Estimators.

The fits obtained from the 29 equations indicate that the *RMSE* values range between 6.43 and 14.34 cm, with models M29, M27, and M22 having the lowest values (Table 3). R^2ajd varies between 0.885 and 0.427, with models M29, M27 and M22 again having the highest values (>0.88). Finally, the *Akaike* criterion values range between 257.53 and 364.13, with models M27, M1, and M29 having the lowest *AIC* values (<258) (Table 3).

Table 3. Fit statistics of the models evaluated to estimate normal diameter from LiDAR data.

Model	*RMSE*	*RMSE* score	R^2ajd	R^2ajd score	*AIC*	*AIC* score	Overall score
M1	6.52	4	0.882	4	257.85	2	10
M2	9.44	22	0.752	22	307.26	22	66
M3	14.34	29	0.427	29	364.13	29	87
M4	10.04	23	0.719	23	315.64	23	69
M5	9.33	21	0.757	21	306.61	21	63
M6	7.30	8	0.851	8	273.34	8	24

M7	8.95	20	0.777	20	300.99	20	60
M8	7.31	9	0.851	9	274.49	9	27
M9	8.48	17	0.799	17	292.76	17	51
M10	11.03	24	0.661	24	328.49	24	72
M11	13.72	28	0.475	28	358.09	28	84
M12	8.30	16	0.808	16	290.81	16	48
M13	6.67	6	0.876	6	261.00	5	17
M14	11.10	25	0.656	25	330.33	25	75
M15	6.65	5	0.877	5	261.56	6	16
M16	8.64	19	0.792	19	295.28	19	57
M17	13.45	27	0.495	27	355.44	26	80
M18	8.00	13	0.822	13	284.72	13	39
M19	8.12	14	0.816	14	287.77	14	42
M20	6.70	7	0.875	7	261.71	7	21
M21	7.73	11	0.833	11	281.13	11	33
M22	6.49	3	0.883	3	258.18	4	10
M23	8.50	18	0.799	18	293.98	18	54
M24	13.41	26	0.498	26	355.99	27	79
M25	7.81	12	0.830	12	282.52	12	36
M26	8.19	15	0.813	15	289.91	15	45
M27	6.46	2	0.884	2	257.53	1	5
M28	7.42	10	0.847	10	276.39	10	30
M29	6.43	1	0.885	1	257.93	3	5

RMSE = Root Mean Square Error; R^2ajd = Coefficient of determination adjusted; *AIC* = Akaike information criterion.

When considering models with a single explanatory variable, those that include *CDL* have the best fit statistics, followed by those that include *THL*. When considering models with two variables, models that consider the joint inclusion of *THL* and *CDL*

have better fit values, which is consistent with the findings of Bi et al. (2012) and Islas-Gutiérrez et al. (2023). The inclusion of *BSHL* as a variable alongside *THL* or *CDL* does not improve the statistical fit of the models, which is why it is considered a variable with low predictive value in modeling *ND* from LiDAR data. Of the models that consider all three variables, M29 has the best statistics, followed by M22.

In a general comparison of the 29 models, M27 and M29 present the best overall score of all (Table 3). The M27 model has the lowest *AIC*, which is a useful criterion for comparing models with different numbers of variables (Fox, 2015), although it has lower *RMSE* and R^2ajd values. The M1 and M22 follow, with values very close to the two previously mentioned models. The M22 has a lower *RMSE* and a higher R^2ajd, while the M1 model has a lower *AIC* because it is a 3-parameter model, while the M22 model has four parameters.

Total height is a widely used variable in modeling height-normal diameter relationships in conifers (Mehtätalo et al., 2015), which is also reflected in the importance of this variable in modeling *ND* with LiDAR data. Meanwhile, crown diameter, although not as widely used in modeling normal diameter, presents a plausible biological relationship with normal diameter (Coombes et al., 2019).

When analyzing the compliance with the regression assumptions of the two best-fitting models (M27 and M29), it is observed that in both, the errors have a normal distribution and constant variance, as judged by the values of the Shapiro-Wilk and Breusch-Pagan tests (Table 4). Regarding the significance tests of the regression estimators, the b_3 of M29 is observed to be non-significant ($p<0.05$) (Table 4). Therefore, it is concluded that M27 is the best option of the different evaluated models.

Table 4. Values and significance tests of the estimators and normality test of the residuals of models M27 and M29.

Mod.	Par.	Est.	*t*-value	*Pr>|t|*	*Shapiro-Wilk* *p*-value	*Breusch-Pagan* *p*-value
M27	β_0	104.318	2.91	0.005	0.516	0.635
	β_1	-3.676	-3.51	0.0008		
	β_2	-0.036	-2.36	0.0215		
	β_3	-0.100	-1.82	0.0491		
M29	β_0	104.489	3.17	0.0024	0.507	0.807
	β_1	-3.801	-3.57	0.0007		
	β_2	-0.044	-2.28	0.0257		
	β_3	0.010	1.16	0.2519		
	β_4	-0.095	-2.01	0.0484		

Mod. = Model; Par. = Parameter; Est. = Estimator; β_0, β_1, β_2, β_3 and β_4 = Model parameters.

The R^2ajd value of the M27 model is higher than those reported by Verma et al. (2014) (R^2=0.68) for five species of the *Eucalyptus* L'Hér. genus in Australia who used the projection of the canopy area as an independent variable, those found by Oono and Tsuyuki (2018) for the Japanese cedar (*Cryptomeria japonica* (Thunb. *ex* L. f.) D. Don) (R^2ajd=0.7301) and for the Japanese cypress (*Chamaecyparis obtusa* (Siebold & Zucc.) Endl.) (R^2ajd =0.7433) with three LiDAR variables as predictors of *ND*, those found by Fu et al. (2018) in the four models they analyzed (R^2<0.53), as well as those obtained by Islas-Gutiérrez et al. (2023) (R^2ajd=0.8781).

Based on all the statistical criteria mentioned above, the M27 model is considered the most appropriate for estimating the *ND* of individual *P. hartwegii* trees using the variables *THL* and *CDL*.

Table 5 shows the results of the M27 validation. In this regard, Koo and Li (2016) indicate that both the point value and the confidence interval should be considered for interpreting the *ICC*. In this case, the *ICC* value is 0.9 and the lower limit of the confidence interval is less than 0.9, leading to the conclusion that the model has good reliability. Regarding the difference of means test, there is no evidence to reject the null hypothesis of equality, which strengthens the conclusion that the model estimates are adequate for calculating normal diameter from total height and crown diameter obtained from LiDAR data.

Table 5. Intraclass correlation coefficient and paired-sample *t*-test for the validation of the M27 model.

	95 % confidence interval		***t*-test**		
ICC	**Lower limit**	**Upper limit**	***t*-value**	**Df**	***p*-value**
0.9	0.752	0.962	-0.91	16	0.3763

ICC = Intraclass correlation coefficient; Df = Degree of freedom.

Conclusions

r>0.9 values obtained between field and LiDAR data for the variables total height, bare stem height, and crown diameter, confirming the usefulness of LiDAR data in supporting forest inventories. Of the 29 models evaluated to estimate the *ND* of *Pinus hartwegii* from LiDAR data, 16 had R^2ajd>0.8 and *RMSE*<8 cm. Models M27

and M29, which are adaptations of the Gompertz model, showed the best values for the R^2ajd, *RMSE* and *AIC* used to select the model. Model M27 was selected because the b_3 estimator of model M29 was not significant. The M27 model is robust enough to estimate the normal diameter of individual *Pinus hartwegii* trees from total height and crown diameter measured on LiDAR data, with a *RMSE* less than 6.5 cm and an R^2ajd of 0.884. Validation of the model using the Intraclass correlation coefficient and a test of means for paired data indicates that its estimates are adequate for calculating *ND*. The results of this study show the high potential of LiDAR data for estimating *ND* to support operational inventories.

Acknowledgments

The authors wish to express their gratitude to the *Instituto Nacional de Investigaciones Forestales*, *Agrícolas y Pecuarias* (*INIFAP*) (National Institute of Forest, Agriculture and Livestock Research) for their support in carrying out this research project from which the information documented in this article originated.

Conflict of Interest

The authors declare no conflict of interest.

Contribution by author

Fabián Islas-Gutiérrez: research conceptualization, data collection and analysis, manuscript preparation and review; Vidal Guerra-De la Cruz, Hugo Ramírez-Maldonado and Enrique Buendía-Rodríguez: data analysis, preparation and review of the manuscript; Tomás Pineda-Ojeda and Eulogio Flores-Ayala: data collection and review of the manuscript.

References

Allouis, T., Durrieu, S., Véga, C., & Couteron, P. (2013). Stem volume and above-ground biomass estimation of individual pine trees from LiDAR data: Contribution of full-waveform signals. *IEEE Journal of Selected Topics in Applied Earth Observations and Remote Sensing*, *6*(2), 924-934. https://www.researchgate.net/publication/236847673_Stem_Volume_and_Above-Ground_Biomass_Estimation_of_Individual_Pine_Trees_From_LiDAR_Data_Contribution_of_Full-Waveform_Signals

Ancira-Sánchez, L., y Treviño-Garza, E. J. (2015). Utilización de imágenes de satélite en el manejo forestal del noreste de México. *Madera y Bosques*, *21*(1), 77-91. http://doi.org/10.21829/myb.2015.211434

Bi, H., Fox, J. C., Li, Y., Lei, Y., & Pang, Y. (2012). Evaluation of nonlinear equations for predicting diameter from tree height. *Canadian Journal of Forest Research*, *42*(4), 789-806. http://doi.org/10.1139/X2012-019

Comisión Nacional de Áreas Naturales Protegidas. (2013). *Programa de Manejo Parque Nacional Iztaccíhuatl Popocatépetl* [Libro blanco]. Secretaría de Medio Ambiente y Recursos Naturales.

https://www.conanp.gob.mx/que_hacemos/pdf/programas_manejo/2014/IZTA_POPO_2014.pdf

Coombes, A., Martin, J., & Slater, D. (2019). Defining the allometry of stem and crown diameter of urban trees. *Urban Forestry & Urban Greening*, *44*, Article 126421. https://doi.org/10.1016/j.ufug.2019.126421

Fau, C., Nabzo, S., y Nasabun, V. (2020). Bondad de ajuste y análisis de concordancia. *Revista Mexicana de Oftalmología*, *94*(2), 100-102. https://www.scielo.org.mx/scielo.php?script=sci_arttext&pid=S2604-12272020000200100

Fox, J. (2015). *Applied regression analysis and generalized linear models* (3rd ed.). Sage Publications, Inc. https://uk.sagepub.com/en-gb/eur/applied-regression-analysis-and-generalized-linear-models/book237254

Fu, L., Liu, Q., Sun, H., Wang, Q., Li, Z., Chen, E., Pang, Y., Song, X., & Wang, G. (2018). Development of a system of compatible individual tree diameter and aboveground biomass prediction models using error-in-variable regression and airborne LiDAR data. *Remote Sensing*, *10*(2), Article 325. https://doi.org/10.3390/rs10020325

Galvincio, J. D., & Popescu, S. C. (2016). Measuring individual tree height and crown diameter for mangrove trees with airborne Lidar data. *International Journal of Advanced Engineering, Management and Science*, *2*(5), 431-443. https://ijaems.com/detail/measuring-individual-tree-height-and-crown-diameter-for-mangrove-trees-with-airborne-lidar-data/

Guo, Q., Su, Y., Hu, T., Guan, H., Jin, S., Zhang, J., Zhao, X., Xu, K., Wei, D., Kelli, M., & Coops, N. C. (2021). Lidar boosts 3D ecological observations and modelings: A review and perspective. *IEEE Geoscience and Remote Sensing Magazine*, 9(1), 232-257. https://doi.org/10.1109/MGRS.2020.3032713

Hall, R. J., Morton, R. T., & Nesby, R. N. (1989). A comparison of existing models for DBH estimation from large-scale photos. *The Forestry Chronicle*, *65*(2), 114-120. http://doi.org/10.5558/tfc65114-2

Hernández, F. J., Meraz-Aragón, J. C., Vargas-Larreta, B., & Nájera-Luna, J. A. (2020). Diameter, height, basal area and volume growth of three pine species from *Chihuahua*, Mexico. *Revista Mexicana de Ciencias Forestales*, *11*(60), 120-143. https://doi.org/10.29298/rmcf.v11i60.711

Hernández-Cuevas, M., Santiago-García, W., De los Santos-Posadas, H. M., Martínez-Antúnez, P., & Ruiz-Aquino, F. (2018). Modelos de crecimiento en altura dominante e índices de sitio para *Pinus ayacahuite* Ehren. *Agrociencia*, *52*(3), 437-453. https://agrociencia-colpos.org/index.php/agrociencia/article/view/1680

Hernández-Ramírez, V., López-Mata, L., Cruz-Rodríguez, J. A., y Luna-Cavazos, M. (2022). Nicho de regeneración de *Abies religiosa* (Kunth) Schltdl. & Cham. en el Monte Tláloc, Parque Nacional Iztaccíhuatl-Popocatépetl, México. *Botanical Sciences*, *100*(2), 331-344. http://doi.org/10.17129/botsci.2912

Hulshof, C. M., Swenson, N. G., & Weiser, M. D. (2015). Tree height–diameter allometry across the United States. *Ecology and Evolution*, *5*(6), 1193-1204. http://doi.org/10.1002/ece3.1328

Islas-Gutiérrez, F., Guerra-De la Cruz, V., Buendía-Rodríguez, E., Pineda-Ojeda, T., Flores-Ayala, E., y Cruz-Juárez, E. (2023). Ecuación para estimar el diámetro normal de árboles individuales de *Pinus hartwegii* Lindl. con datos LiDAR. *Revista Tecnológica CEA*, *8*(23), 515-521. https://revistatecnologicacea.mx/revista22/

Koo, T. K., & Li, M. Y. (2016). A guideline of selecting and reporting intraclass correlation coefficients for reliability research. *Journal of Chiropractic Medicine*, *15*(2), 155-163. http://dx.doi.org/10.1016/j.jcm.2016.02.012

Lara-Vásconez, N., y Chamorro-Sevilla, H. (2018). Uso de los sensores remotos en mediciones forestales. *European Scientific Journal*, *14*(15), 58-77. http://doi.org/10.19044/esj.2018.v14n15p58

Liu, W., Zhong, T., & Song, Y. (2017). Prediction of trees diameter at breast height based on unmanned aerial vehicle image analysis. *Transactions of the Chinese Society of Agricultural Engineering*, *33*(21), 99-104. http://doi.org/10.11975/j.issn.1002-6819.2017.21.012

Ma, L., Liu, Y., Zhang, X., Ye, Y., Yin, G., & Johnson, B. A. (2019). Deep learning in remote sensing applications: A meta-analysis and review. *ISPRS Journal of Photogrammetry and Remote Sensing*, *152*, 166-177. https://doi.org/10.1016/j.isprsjprs.2019.04.015

Martínez-Pérez, J. A., y Pérez-Martín, P. S. (2023). Coeficiente de correlación intraclase. *Medicina de Familia SEMERGEN*, *49*(3), Article 101907. https://doi.org/10.1016/j.semerg.2022.101907

McGaughey, R. J. (2024). *FUSION/LDV: Software for LIDAR Data Analysis and Visualization. FUSION Version 4.61*. United States Department of Agriculture. https://forsys.sefs.uw.edu/software/fusion/FUSION_manual.pdf

Mehtätalo, L., de-Miguel, S., & Gregoire, T. M. (2015). Modeling height-diameter curves for prediction. *Canadian Journal of Forest Research*, *45*(7), 826-837. http://doi.org/10.1139/cjfr-2015-0054

Montes de Oca-Cano, E., Salvador-García, Á., Nájera-Luna, J. A., Corral-Rivas, S., Graciano-Luna, J. de J., y Méndez-González, J. (2020). Ecuaciones alométricas para estimar biomasa y carbono en *Trichospermum mexicanum* (DC.) Baill. *Colombia Forestal*, *23*(2), 89-98. https://doi.org/10.14483/2256201x.15836

Ng'andwe, P., Chungu, D., Yambayamba, A. M., & Chilambwe, A. (2019). Modeling the height-diameter relationship of planted *Pinus kesiya* in Zambia. *Forest Ecology and Management*, *447*, 1-11. http://doi.org/10.1016/j.foreco.2019.05.051

Ogana, F. N. (2019). Modelling crown-stem diameters relationship for the management of *Tectona grandis* Linn f. plantation in Omo Forest Reserve, Western

Nigeria. *Annals of Silvicultural Research*, *43*(2), 89-96. https://doi.org/10.12899/asr-1865

Oono, K., & Tsuyuki, S. (2018). Estimating individual tree diameter and stem volume using airborne LiDAR in Saga Prefecture, Japan. *Open Journal of Forestry*, *8*(2), 205-228. http://doi.org/10.4236/ojf.2018.82015

Ott, R. L., & Longnecker, M. (2010). *An introduction to statistical methods and data analysis* (6th ed.). Cengage Learning Inc. http://repository.bitscollege.edu.et:8080/bitstream/handle/123456789/789/LYMANO~1.PDF?sequence=1

Pérez-Suárez, M., Ramírez-Albores, J. E., Vargas-Hernández, J. J., & Alfaro-Ramírez, F. U. (2022). A review of the knowledge of Hartweg´s pine (*Pinus hartwegii* Lindl.): current situation and the need for improved future projections. *Trees*, *36*, 25-37. http://doi.org/10.1007/s00468-021-02221-9

QGIS Development Team. (2024). *QGIS Geographic Information System* (version 3.42) [Software]. Open Source Geospatial Foundation Project. http://qgis.osgeo.org

R Core Team. (2025). *The R Project for Statistical Computing* (version 4.4.3) [Software]. R Foundation for Statistical Computing. https://www.R-project.org/

Reutebuch, S. E., Andersen, H.-E., & McGaughey, R. J. (2005). Light detection and ranging (LIDAR): An emerging tool for multiple resource inventory. *Journal of Forestry*, *103*(6), 286-292. https://www.fs.usda.gov/pnw/pubs/journals/pnw_2005_reutebuch001.pdf

SAS Institute Inc. (2011). *SAS Version 9.3* [Software]. SAS Institute Inc. https://www.sas.com/en_us/home.html

Shiota, H., Tanaka, K., & Nagashima, K. (2017). LiDAR data analysis with Fusion/LDV for individual tree measurement. *Journal of Biodiversity Management and Forestry*, *6*(3), 1-8. http://doi.org/10.4172/2327-4417.1000184

Tamarit-Urías, J. C., De los Santos-Posadas, H. M., Aldrete, A., Valdez-Lazalde, J. R., Ramírez-Maldonado, H., y Guerra-De la Cruz, V. (2014). Sistema de cubicación

para árboles individuales de *Tectona grandis* L. f. mediante funciones compatibles de ahusamiento-volumen. *Revista Mexicana de Ciencias Forestales*, *5*(21), 58-74. http://doi.org/10.29298/rmcf.v5i21.358

Valverde, J. C., Rubilar, R., Medina, A., Mardones, O., Emhart, V., Bozo, D., Espinoza, Y., & Campoe, O. (2022). Taper and individual tree volume equations of *Eucalyptus* varieties under contrasting irrigation regimes. *New Zealand Journal of Forestry Science*, *52*, Article 15. http://doi.org/10.33494/nzjfs522022x181x

Verma, N. K., Lamb, D. W., Reid, N., & Wilson, B. (2014). An allometric model for estimating DBH of isolated and clustered Eucalyptus trees from measurements of crown projection area. *Forest Ecology and Management*, *326*, 125-132. http://doi.org/10.1016/j.foreco.2014.04.003

Wang, R., & Gamon, J. A. (2019). Remote sensing of terrestrial plant biodiversity. *Remote Sensing of Environment*, *231*, Article 111218. https://doi.org/10.1016/j.rse.2019.111218

Yang, Z., Liu, Q., Luo, P., Ye, Q., Duan, G., Sharma, R. P., Zhang, H., Wang, G., & Fu, L. (2020). Prediction of individual tree diameter and height to crown base using nonlinear simultaneous regression and airborne LiDAR data. *Remote Sensing*, *12*(14), Article 2238. https://doi:10.3390/rs12142238

Zhang, Z., Wang, T., Skidmore, A. K., Cao, F., She, G., & Cao, L. (2023). An improved area-based approach for estimating plot-level tree DBH from airborne LiDAR data. *Forest Ecosystems*, *10*, Article 100089. http://doi.org/10.1016/j.fecs.2023.100089